
Article:
Hussein, AT and Elmirghani, J (2015) 10 Gbps Mobile Visible Light Communication System Employing Angle Diversity, Imaging Receivers, and Relay Nodes. IEEE/OSA Journal of Optical Communications and Networking, 7 (8). 718 - 735. ISSN: 1943-0620

https://doi.org/10.1364/JOCN.7.000718

---

10 Gbps Mobile Visible Light Communication System Employing Angle Diversity, Imaging Receivers and Relay Nodes

Ahmed Taha Hussein and Jaafar M.H. Elmirghani

Abstract—Over the last decade, visible light communication (VLC) systems have typically operated between 50 Mbps and 3.4 Gbps. In this paper, we propose and evaluate mobile VLC systems that operate at 10 Gbps. The enhancements in channel bandwidth and data rate are achieved by the introduction of laser diodes (LDs), angle diversity receivers (ADR), imaging receivers, relay nodes and delay adaptation techniques. We propose three mobile VLC systems; an ADR relay assisted LD-VLC (ADRR-LD), an imaging relay assisted LD-VLC (IMGR-LD) and select-the-best imaging relay assisted LD-VLC (SBIMGR-LD). The ADR and imaging receiver are proposed for the VLC system to mitigate the intersymbol interference (ISI), maximise the signal to noise ratio (SNR) and reduce the impact of multipath dispersion due to mobility. The combination of IMGR-LD with a delay adaptation technique adds a degree of freedom to the link design, which results in a VLC system that has the ability to provide high data rates under mobility. The proposed IMGR-LD system achieves significant improvements in the SNR over other systems in the worst case scenario in the considered real indoor environment.

***Index Terms*— Angle diversity receiver, imaging receiver, relay nodes, delay adaptation technique, SNR.**

I. INTRODUCTION

In the near future, indoor wireless systems will be required to offer multi-gigabit per second connectivity. Optical wireless (OW) systems are candidates for high data rates in last mile network access. It has been more than three decades since the first OW systems were proposed as an alternative technology to radio frequency systems to support high data rates [1]. One of the most promising OW systems for realising ubiquitous wireless networks is visible light communication (VLC) based on white light emitting diodes (LEDs), since LEDs can be used for both illumination and data communications, simultaneously [2]. The dual functionality of a VLC, i.e. illumination and communication, makes it a very attractive technology for many indoor and outdoor applications such as car-to-car communication via LEDs, employing lighting infrastructures in buildings for high speed data communication and high data rate communication in airplane cabins. However, the traditional VLC system suffers from limitations in the modulation bandwidth of the transmitters (i.e. LEDs) [3]. Therefore, alternative transmitters are needed for VLC systems to achieve high data rates.

The main challenges hindering the development of a VLC system are the low modulation bandwidth of the LEDs and intersymbol interference (ISI). The modulation bandwidth available in the transmitters (LEDs) is typically less than the VLC channel bandwidth, which means that the former typically limits the transmission rates. A number of solutions have been suggested to achieve high data rates in the VLC system. Among the most notable solutions is the use of optical filters, pre- or post-equalization [4] (or both), complex multiple access and modulation techniques [5] as well as parallel communication [6] (i.e. optical multiple input multiple output-OMIMO) and red, green and blue (RGB) LEDs [7]. The MIMO VLC channel has been used to improve the data rate under illumination constraints [8]. Pulse position modulation has been jointly used with the MIMO approach to enhance the data rates without reducing the reliability of the link in [9]. Colour shift keying (CSK) was proposed for increasing data throughput by encoding data in the instantaneous output colour of the LEDs [10]. A 1.25 Gbps system was reported in [7] using RGB LEDs in a single colour transmission mode, and 1.5 Gbps has been achieved using a new design of μLED array that incorporates non-return-to-zero On-Off Keying (NRZ-OOK) as a modulation scheme. The 3 dB modulation bandwidth of this μLED was 150 MHz [11]. Higher data rates can be achieved using wavelength division multiplexing (WDM) with RGB LEDs. The highest throughput achieved using LEDs was reported in [12], where the aggregate throughput was 3.4 Gbps when using discrete multi-tone modulation (DMT), WDM and RGB LEDs. The design and implementation complexity are a major concern in these systems.

Manuscript received March 18, 2015.

A. T. Hussein is with the School of Electronic and Electrical Engineering, University of Leeds, Leeds LS2 9JT, U.K. (e-mail: ml12ath@leeds.ac.uk).

J. M. H. Elmirghani is with the School of Electronic and Electrical Engineering, University of Leeds, Leeds LS2 9JT, U.K. (e-mail: j.m.h.elmirghani@leeds.ac.uk).

Conventional VLC systems have used organic LEDs and RGB LEDs as transmitters. However, due to their low modulation bandwidth, the highest VLC throughput (3.4 Gbps) achieved by LEDs, to the best of our knowledge, was reported in [12]. Therefore, significant research effort is being directed towards increasing the modulation bandwidth of the LEDs. Micro LEDs (μLED) have been proposed for use in VLC systems to enable them to achieve 3 Gbps [13]. Potentially, 10 Gbps data rates could be delivered with an RGB triplet in such devices [13]. The high modulation bandwidth transmitter in the VLC system is vital to achieve high data rates. Therefore, we have suggested the use of laser diodes (LDs), which can operate at the Gbps range. This figure means that LDs can be attractive VLC transmitters. However, in general LDs are not very popular for illumination purposes due to potential health hazards, cost, colour mixing complexity and the spectral emission profile of a typical LD, which is in the order of 2−3 nm and their spot size is very narrow compared to LEDs. Nevertheless, a recent study has demonstrated that diffused laser light does not compromise the user experience compared with conventional LEDs [14]. BMW introduced laser light in their i8 model. This system uses blue lasers and phosphors to generate white light [15]. Recently, different types of RGB LD lights have been investigated to generate white light [16]. One of the main potential issues associated with using laser lighting is that lasers can be dangerous to human eyes. However, it should be noted that while the original sources indeed have laser source properties, once they have been combined and had the beam scattered and diffused, the light no longer has the characteristics of laser light, but resembles white light [17], [18], which meets illumination safety standards. This white light has exactly the same characteristics (e.g. colour rendering) of white light that is produced from LEDs, as experimental results have shown [14] (see table I in [14]). The authors in [16] have experimentally proved that RGB LDs have comparable characteristics to a white LED source. An illumination infrastructure (a communication network and control systems) can be used to support a number of LD light engines in a building, and their illumination can be controlled via plastic fibre optic cables that can be run along the ceiling. A good example for such a system is the LD light source introduced by Toshiba [19]. A combination of RGB visible lasers with a diffuser can be used to generate white light that has high quality colour rendering and efficiency [20]. Therefore, it is expected that visible laser diodes (LDs) can be used as a source of illumination instead of LEDs due to their high efficiency, especially in high power applications [18], [21]. Recently, the authors in [22] projected that laser-produced illumination, if cost effective, could enable significant performance gains in VLC systems due to the high frequency modulation capabilities of lasers.

In our previous work, we used RGB-LDs to provide illumination as well as acting as a transmitter instead of LEDs in a VLC system [23], [24]. Thus, the main challenge in the traditional VLC system (i.e. the low modulation bandwidth of LEDs) can be tackled.

VLC links can be classified into two basic schemes: line of sight (LOS) and non-LOS (NLOS). LOS links provide a direct path between transmitter and receiver, minimise multipath dispersion and enhance the power efficiency of the VLC communication system. However, LOS links suffer from shadowing. On the other hand, NLOS links rely on reflections from the walls, ceiling and other objects. They offer robust links and protection against shadowing but they are severely affected by multipath dispersion, which results in ISI and pulse spread [2], [25]. In a VLC system, LOS can be achieved with many light units on the ceiling. However, the optical path differences between light units result in ISI. In this work, both LOS and NLOS links are considered.

In the literature, many techniques for VLC systems have been proposed to mitigate ISI. Among the most notable solutions is the use of adaptive equalization using the least mean square algorithm which has the ability to reduce the effects of ISI and was investigated at data rates up to 1 Gbps [26]. The authors in [27] used MIMO techniques to reduce shadowing effects. Orthogonal frequency division multiplexing (OFDM) can be used in a VLC system just as in traditional wireless systems to reduce the effects of ISI [28]. The authors in [29] used zero forcing (ZF) equalization with such transmitter arrangements to reduce the effects of ISI. The achieved bit error rate (BER) with this technique was similar to the channel without ISI.

An angle diversity receiver (ADR) and an imaging receiver are solutions that can tackle the signal spread caused by multipath in a VLC system [3], [30], [31]. A three branch ADR with RGB LD has been proposed in [24], and 5 Gbps was achieved in an empty room. Our previous work in this area has shown that significant enhancements can be achieved when using an imaging receiver [23]. The data rate achieved by this previously developed VLC system was 5 Gbps by introducing a LD and imaging receiver [23].The main limitations in the traditional VLC system (i.e. the low modulation bandwidth of the LEDs and ISI) have been addressed previously by using LDs instead of LEDs and the wide field of view (FOV) receiver has been replaced by the imaging receiver which has narrow FOV pixels [23]. The data rate achieved by this previously developed VLC system was 5 Gbps in the worst case scenario [23]. However, its link performance was negatively affected by mobility and this leads to performance degradation in the signal to noise ratio (SNR) and channel bandwidth. Therefore, in this paper we introduce the concept of relay assisted VLC systems to improve the overall system performance.

Relays have been previously considered for use in different networks to reduce the transmission distances and increase system capacity [32], [33]. Relays were introduced by Meulen in 1971 [34] and spread widely in radio communication after the emergence of the cooperative communication idea [33].

In the literature, relay assisted free space optical (FSO) wireless systems have been proposed and studied in different modes: amplify and forward (AF), and decode and forward (DF) [35], [36]. Relays were used in FSO system to provide multi-hop diversity to the destination. In [37] an LED light bulb in a desk lamp is used as a relay when it receives a radio signal from a mobile device and broadcasts it back to the desk with larger coverage and higher light intensity. In an infrared OW system the concept of relays is studied in [38]. The use of intermediate nodes in OW systems can lead to significant improvements in SNR and considerable extra bandwidth in the channel. Relays can either be idle users present in the communication floor who

can cooperate in the transmission, or they can be transceivers deployed solely for this purpose [38].

In this paper three new VLC systems, an ADR relay assisted LD-VLC (ADRR-LD), an imaging relay assisted LD-VLC (IMGR-LD) and select-the-best imaging relay assisted LD-VLC (SBIMGR-LD) are modelled and their performance is compared at 10 Gbps in two VLC room sizes (5×5×3 m^3 and 4×8×3 m^3). We also model two different room scenarios: an empty room and a real environment room that has a door, windows, bookshelves, mini cubicles and other objects. The challenge in both rooms is the ability to establish LOS communication link between transmitter and receiver at all relevant locations. We have used the previously introduced LDs, delay adaptation and imaging receiver, and we have achieved 10 Gbps in a realistic environment, which is a 2x increase in data rate compared with [23] and [24], and in the current work we introduce the concept of relays in VLC systems for the first time. The main difference between the proposed VLC systems in this study and traditional VLC systems is the use of RGB LDs as the transmitters instead of LEDs. The main advantage of using visible LDs is their wide modulation bandwidths ranging from hundreds of MHz to more than 10 GHz. Thus, multi gigabit per second VLC systems can be realized with the simple modulation format (OOK) and without the use of relatively complex wavelength division multiplexing approaches.

The remainder of this paper is organised into the following sections: Section II presents LD light design; Section III presents the simulation environment and VLC channel model; Section IV describes the receivers' configurations. Section V presents the proposed VLC systems' configurations. Section VI provides the simulation results and discussion of the ADRR-LD system, IMGR-LD system and SBIMGR-LD system in an empty room. Section VII presents the simulation results and discussion of the proposed systems in a small office environment. The robustness of the proposed systems against mobility, shadowing and signal blockage is investigated in Section VIII. Finally, conclusions are drawn in Section IX.

II. LD Light Design

The primary function of the LD is illumination, so it is essential to clarify the luminous intensity. To achieve comfortable office lighting, 300 lx is considered to be the minimum requirement for illumination, according to the European standard EN 12464-1 [39]. The brightness of the LD is expressed as luminous intensity. Luminous intensity is the luminous flux per solid angle as defined in [40]:

$$I = \frac{d\emptyset}{d\Omega} \tag{1}$$

where Ω is the spatial angle and $\emptyset$ is the luminous flux. From the energy flux (emission spectrum) $\emptyset e$, $\emptyset$ can be calculated as in [40]:

$$\emptyset = F \int_{380}^{780} A(\lambda)\, \emptyset e\,(\lambda)\, d\lambda \tag{2}$$

where $A(\lambda)$ is the eye sensitivity function and F is the maximum visibility, which is equal to 683 lm/W at a 555 nm wavelength. Assuming that the LD light has a Lambertian radiation pattern, the direct LOS horizontal illumination at any point in the office can be calculated as [40]:

$$E_{hor} = (0)\frac{cos^n(\theta)\, cos(\gamma)}{D_d^2} \tag{3}$$

where $I(0)$ is the centre luminous intensity of the LD, θ is the irradiance angle, D_d is the distance between LD and the point of interest, γ is the angle of incidence and n is the Lambertian emission order that can be calculated as [41]:

$$n = -\frac{ln(2)}{ln\left(cos\left(\vartheta_{\frac{1}{2}}\right)\right)} \tag{4}$$

where $\vartheta_{\frac{1}{2}}$ is the semi-angle at half power of the LD.

A combination of RGB lasers with a diffuser can be used to generate white light [20]. Therefore, the room's illumination was provided by eight RGB-LD light units which were used to ensure that ISO and EU standards are satisfied [39]. Each LD light unit has 9 (3×3) RGB-LD. The specifications of the RGB-LDs used in this study were adopted from the practical results reported in [14], where the measured illuminance for each RGB-LD was 193 lx. Therefore, the centre illumination intensity for each RGB-LD was 162 cd. The conversion from illuminance (lx) to luminous intensity (cd) was carried out using the inverse square law which is valid if (i) the source is a point source (ii) the beam is divergent and (iii) the distance of interest is greater than ten times the source size [42]. Fig.1 shows the architecture of the LD light units, where the light from three lasers (i.e. RGB) is combined using beam combiners, then passes through multiple ground glass diffusers to reduce speckle before illuminating the room. This design is similar to one studied in [14]. Beam-splitters and detectors were used to monitor and control (tune LDs light engine) the different laser powers. A few percent of the beam power is needed for that purpose. Changing the power emitted by each laser can be used to obtain the exact colour desired and set the total emitted power.

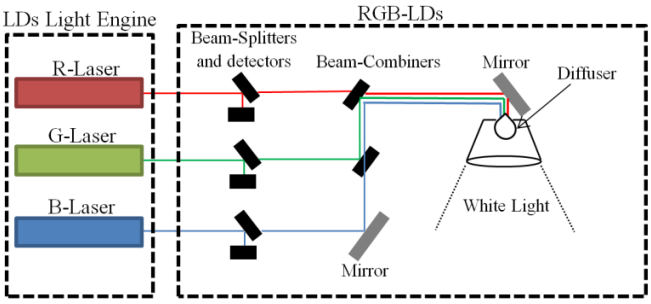

Fig.1: Architecture of RGB-LD illumination system: light from three lasers is combined using chromatic beam-combiners, then passes through multiple ground glass diffusers to reduce speckle before illuminating the room.

III. Simulation Environment and VLC Channel Model

To study the benefits of our techniques for an indoor VLC system, a simulation based on a ray-tracing algorithm was performed in an empty room. The simulation model was developed using room dimensions of 4 m × 8 m (width × length) with a ceiling height of 3 m. The walls, ceiling and floor were modelled as ideal Lambertian reflectors with reflection coefficients of 0.8, 0.8 and 0.3, respectively [1]. It

was shown that plaster walls reflect rays in a form close to a Lambertian function [1]. Therefore, all walls (including the ceiling) and the floor were modelled as Lambertian reflectors.

Room illumination was provided by eight RGB-LD light units. These RGB-LD lights were installed at a height of 3 m above the floor. The transmitted power from each RGB-LD was 2 W. The height of the work desks where the user communication equipment was placed, was 1 m. This horizontal plane was referred to as the "communication floor", (CF). The coordinates of the RGB-LD light units were (1 m, 1 m, 3 m), (1 m, 3 m, 3 m), (1 m, 5 m, 3 m), (1 m, 7 m, 3 m), (3 m, 1 m, 3 m), (3 m, 3 m, 3 m), (3 m, 5 m, 3 m) and (3 m, 7 m, 3 m). A number of different uniformly distributed LD light unit configurations (i.e. 4, 6 and 8 RGB-LD units) were tested in the room to find the optimum number of units that ensures that the ISO and EU illumination requirements are satisfied.

To model the reflections, the room was divided into a number of equal-size (square shaped) reflection elements. Each reflection element was treated as a small transmitter that transmits an attenuated version of the received signals from its centre in the same form as a Lambertian pattern with n =1 (i.e. $\vartheta_{\frac{1}{2}} = 60^{o}$).

Previous research considered reflections up to first order [2], [13], [26]. However, this may not provide a full description of the characteristics of the channel. Therefore, in our simulation, reflections up to second order were considered, since the second order reflection has a great impact on the system performance (especially at high data rates). Surface elements of 5 cm × 5 cm for first-order reflections and 20 cm × 20 cm for second-order reflections were used. These values were selected to keep the computation requirements within reasonable time (the computation time increases dramatically when the surface element size is decreased). Additional simulation parameters are given in Table I. The proposed system's performance under mobility and multipath propagation are evaluated. Three new VLC systems are considered in this work: ADRR-LD, IMGR-LD and SBIMGR-LD systems. All the proposed systems use an upright transmitter at the CF and the transmitter is placed at three different locations on the CF: (1 m, 1 m, 1 m), (2 m, 1 m, 1 m) and (2 m, 4 m,1 m). These transmitter locations represent three main cases: transmitter underneath relay (best case), transmitter between two relays and transmitter at the centre of the room, which is considered the worst case scenario due to the large distance between transmitter and relay.

The simulations and calculations reported in this paper were carried out using MATLAB. Our simulation tool is similar to the one developed by Barry et al. [43], and it is used to produce impulse responses, the power distribution and to calculate the delay spread, 3 dB channel bandwidth and SNR. Fig.2 shows the VLC room with eight RGB-LD light units (eight relays) with upright transmitter and receiver both located on CF.

Fig.3 shows the horizontal illuminance distributions from the eight RGB-LD light units at the CF level. It can be clearly seen that using eight light units was sufficient in terms of illumination as it achieved the required illuminance, i.e. above 300 lx [39]. Therefore, eight light units were used in this study.

In all OW links, including VLC, channel intensity modulation with direct detection (IM/DD) is the preferred choice [41], [44].

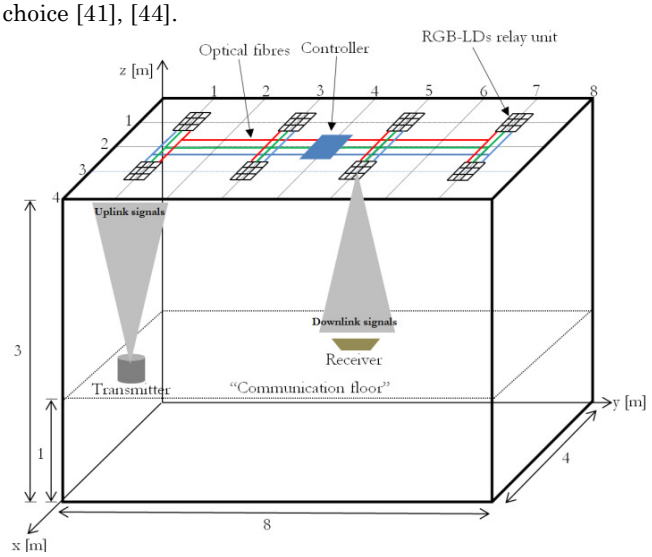

Fig.2: VLC system room.

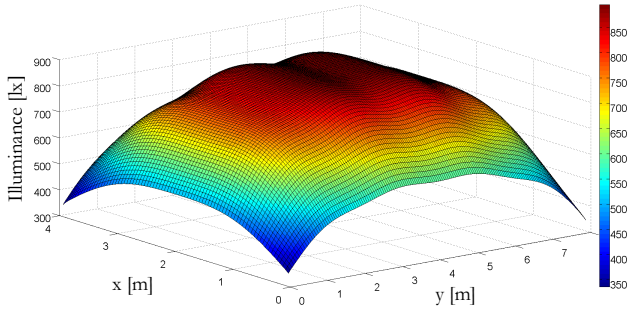

Fig.3: The distribution of horizontal illuminance at the CF, Min.336 lx and Max.894 lx.

The IM/DD channel can be modelled as a baseband linear system. Let $x(t)$ be the input power and $I(t)$ be the photo current received that results from the integral of the received optical power over the photo detector surface. An indoor OW channel that uses IM/DD can be fully characterised by the impulse response of the channel as given in [45], [46]:

$$I(t) = R\, x(t) \otimes h(t) + n_b(t) \tag{5}$$

where R is the photo detector responsivity, t is the absolute time, $\otimes$ denotes convolution, n_b is the background noise (BN), which is modelled as AWGN and $h(t)$ is the impulse response. The received photo-current I_r by the relay can be given as:

$$I_r = R\, P_s\, x(t) \otimes h_{sr}(t) \tag{6}$$

where P_s is the optical power of the transmitter, $h_{sr}(t)$ is the channel response between the transmitter and the relay. The photo-current I_d at the receiver can be written as:

$$I_d = R\left[\left(R\, P_s\, x(t) \otimes h_{sr}(t)\right) \otimes h_{rd}(t)\right] + n_d(t) \tag{7}$$

where $h_{rd}(t)$ is the channel response of the relay-receiver link, and $n_d(t)$ is the noise at the receiver.

TABLE I

SIMULATION PARAMETERS

Parameters	Configurations	
Length	8m	
Width	4m	
Height	3m	
ρ-ceiling	0.8 [1]	
ρ-xz wall	0.8 [1]	
ρ-yz wall	0.8 [1]	
ρ-xz op-wall	0.8 [1]	
ρ-yz op-wall	0.8 [1]	
ρ-floor	0.3 [1]	
Bounces	1	2
Number of elements	32000	2000
dA	5cm×5cm	20cm×20cm
	[31], [38]	
Transmitter		
Number of Transmitters	1	
Locations (x, y, z)	(1,1,1), (2,1,1),(2,4,1)	
Relays		
Number of relays	8	
Locations (x, y, z)	(1,1,3), (1,3,3), (1,5,3), (1,7,3) (3,1,3), (3,3,3), (3,5,3), (3,7,3)	
Elevation	90°	
Azimuth	0°	
Number of RGB-LDs in each transmitter unit	9 (3×3)	
Semi-angle at half power	70°	
Centre luminous intensity	162 cd [14]	
Transmitted optical power of a RGB-LDs	2 W [14]	

Various parameters can be derived from the simulated impulse response, such as the delay spread and 3 dB channel bandwidth. The delay spread is a good measure of the signal pulse spread due to the temporal dispersion of the incoming signal. The delay spread of an impulse response is given by:

$$D = \sqrt{\frac{\sum (t_i - \mu)^2 P_{ri}^2}{\sum P_{ri}^2}} \tag{8}$$

where t_i is the delay time associated with the received optical power P_{ri} and μ is the mean delay given by:

$$\mu = \frac{\sum t_i P_{ri}^2}{\sum P_{ri}^2} \tag{9}$$

IV. Receivers' Configurations

We used two types of receiver, a non-imaging receiver (ADR) and an imaging receiver that employs a single planner array to facilitate the use of a large number of pixels. An ADR is a group of narrow FOV detectors pointed in different directions. The ADR consists of seven branches with photodetectors that have a responsivity of 0.4 A/W. The direction of each branch in an ADR is defined by two angles: the azimuth angle (AZ) and the elevation angle (EL).

The AZs of the seven detectors are set at 0°, 45°, 90°, 135°, 225°, 270° and 315°, and ELs for the seven branches are fixed at 90°, 45°, 60°, 45°, 45°, 60° and 45°. The corresponding FOVs were fixed to 20°, 15°, 25°, 15°, 15°, 25° and 15°. The AZs, ELs and FOVs were chosen through an optimisation process to achieve the best SNR and minimum delay spread.

To compute the reception angle (Φ) for any detector in the ADR, a point P has to be defined (see Fig.4 a), which is located 1 m above the detector. E is an element on the wall with coordinates (x_E, y_E, z_E). Fig.4 (a) shows light from a reflecting point (E) on a wall incident on one of the detectors in the ADR that is located at (x_r, y_r, z_r). Φ can be calculated as [45], [47]:

$$cos(\Phi) = \frac{\left|\overrightarrow{PR_x}^2\right| + \left|\overrightarrow{ER_x}^2\right| - \left|\overrightarrow{E_P}^2\right|}{2\left|\overrightarrow{PR_x}^2\right|\left|\overrightarrow{ER_x}^2\right|} \tag{10}$$

where:

$$\left|\overrightarrow{PR_x}^2\right| = 1 + \left(\frac{1}{tan\, EL}\right)^2 \tag{11}$$

$$\left|\overrightarrow{ER_x}^2\right| = (x_r - x_E)^2 + (y_r - y_E)^2 + (z_r - z_E)^2 \tag{12}$$

$$\left|\overrightarrow{E_P}^2\right| = \left[\left(\frac{cos(AZ)}{tan(EL)} + x_r\right) - x_E\right]^2 + \left[\left(\frac{sin(AZ)}{tan(EL)} + y_r\right) - y_E\right]^2 + [(z_r + 1) - z_E]^2 \tag{13}$$

All photo detectors have same detection area, 4 mm². The ADR is always placed on the CF. We examined the VLC system performance along the two important lines x=1 m and x=2 m. Fig.4 (b) illustrates the physical structure of ADR. The imaging receiver is a potential solution that can mitigate the impact of ISI and provide mobility for the VLC system [23].

Two significant advantages are offered by the imaging receiver over the non-imaging ADR: first, a single planner array is used for all photo-detectors, which can facilitate the use of a large number of pixels. Second, a common imaging concentrator (for example, a lens) can be shared between all photo-detectors, reducing the cost and size compared to other kinds of receiver [48].

The detector array of the imaging receiver is segmented into j equal-sized rectangular shaped pixels, as shown in Fig.5. In this case, and under most circumstances, the signal falls on no more than four pixels [48]. Therefore, the area of each pixel is the photo-detector's area, which is equal to the exit area of the imaging concentrator used divided by the number of pixels. In this study, the detector array was segmented into 50 pixels and the imaging receiver employed a non-imaging concentrator. When the receiver was located at the centre of the room it was designed to see the whole ceiling, and the ceiling was subdivided in this case into 50 segments (5×10 along the x and y axes, respectively), and each reception area or segment was cast onto a single pixel.

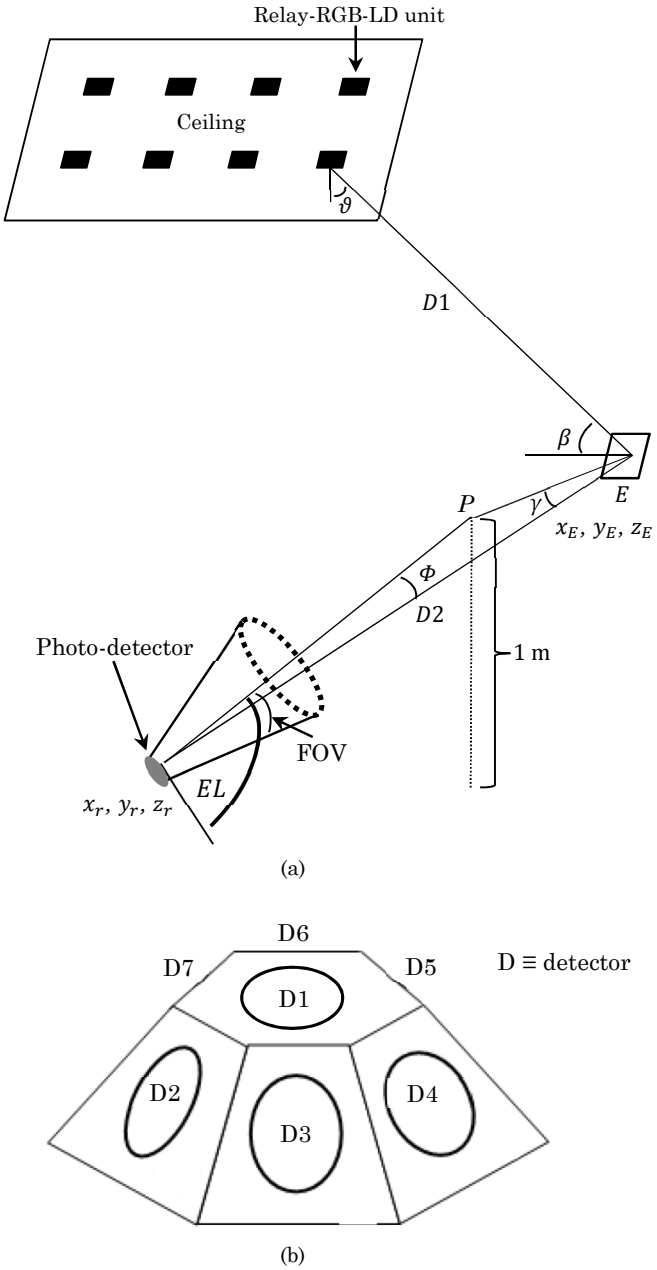

Fig.4: Angle diversity receiver (a) azimuth and elevation parameters of the diversity detection receiver; (b) physical structure of the angle diversity receiver with seven branches.

The imaging receiver employs a compound parabolic concentrator (CPC) that can collect and concentrate the light from a large input area down to a smaller detector area (exit area). The CPC is a non-imaging concentrator that has an acceptance angle of ψ_a<90°. When the reception angle δ exceeds ψ_a the concentrator transmission factor rapidly approaches zero. The CPC has an entrance area $A = \frac{9\pi}{4}$ cm² while the exit area is $A' = \frac{A \sin^2(\psi_a)}{N^2}$, where N is the refractive index (N = 1.7). The concentrator gain $g(\psi a)$ is given by [41]:

$$g(\psi a) = \frac{N^2}{\sin^2(\psi_a)} \quad (14)$$

The transmission factor of the concentrator is given by [49]:

$$T_c(\delta) = -0.1982\delta^2 + 0.0425\delta + 0.8778 \quad (15)$$

where δ is the incidence angle measured in radians. We set the semi-acceptance angle (ψ_a) of this concentrator to 65°, so that it can view the whole ceiling when the receiver is at the centre of the room. The detector array is assumed to fit exactly into its corresponding concentrator's exit area. Therefore, the detector array has a photosensitive area of 2 cm² and each pixel has a particular area of 4 mm². The pixel's reception area calculations are given in detail in [23].

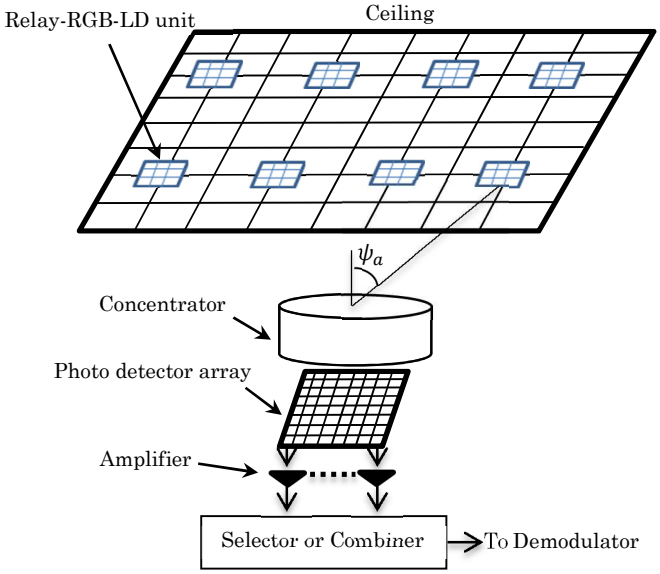

Fig.5: The physical structure of an imaging receiver.

V. Systems' Configurations

In this section, three new VLC systems are presented, analysed and compared in order to identify the most appropriate system for use in multi-gigabit VLC systems.

A. ADRR-LD

The ADRR-LD system employs one upright transmitter on the CF, eight relays (lighting fixtures) on the ceiling connected by fibre interconnects and controlled by a central controller and a seven branch ADR located on the CF as shown in Fig.6a. A communication set up (CS) algorithm is proposed to select the optimum link between transmitter and relays (under mobility, this algorithm can be called periodically). For a single transmitter at a given set of positions, the CS algorithm identifies the optimum link according to the following steps:

1- The controller activates a listening mode in all the relays (eight relays).
2- The transmitter on the CF sends a pilot signal.
3- SNR is computed at each relay.
4- The relay that yields the best SNR is chosen by the controller (which is mostly the closest relay to the transmitter).
5- The controller deactivates the remaining seven relays and keeps the closest relay 'ON'.
6- The closest relay sends a feedback signal to the transmitter to start operating mode (i.e. start sending information signals).

It should be noted that the RGB-LD light units (i.e. relays) should always be 'ON' to provide illumination for the room. Therefore, to prevent flickering, an OOK dimming technique may be used [50].

Once the information signals are sent by the transmitter, the closest relay to the transmitter receives it and the controller broadcasts the information to the rest of the relays to start transmission to the destination (ADR). Switching 'ON' the relays and emitting signals simultaneously from the relays (light fixtures) may result in receiving the signals at different times due to multipath propagation. Therefore, a delay adaptation technique (DAT) is coupled with the ADRR-LD system to enhance the SNR and channel bandwidth. The delay adaptation technique was previously proposed in [23]. It adjusts the switching times of the signals as follows:

1- A pilot signal is sent from the first relay.
2- The mean delay (μ) at the receiver for the first relay unit is estimated at the receiver side by branch 1 of the ADR.
3- Repeat step 2 for the other branches in the ADR.
4- Repeat steps 2 and 3 for the other relay units.
5- The receiver sends a control feedback signal to inform the controller of the associated delay with each received signal from each relay.
6- The controller introduces a differential delay (Δt) between the signals transmitted from the relays.
7- The relay units send signals according to the delay values such that a relay unit that has the largest delay, i.e. longest path to the receiver, transmits first.

A speed of 1 m/s is typical for indoor users, we therefore propose that the CS algorithm and delay adaptation technique re-estimate SNR and delay values at the start of a 1-second frame, and if these have changed compared to the previous frame values then the receiver uses the feedback channel to update the controller. If the time taken to determine the value of each SNR and delay associated with each relay (relative to the start of the frame) is equal to 1 ms (based on typical processor speeds), then our CS algorithm and delay adaptation method training time is 80 ms (8 relays × 1 ms + 9 RGB-LDs in each relay unit × 8 relay units × 1 ms). This rate (80 ms, once every 1-second frame) is sufficient given that the CS and delay adaptation have to be carried out at the rate at which the environment changes (pedestrian movement). Therefore, the adaptive system can achieve 100% of the specified data rate when it is stationary, and 92% in the case of transmitter or user movement, i.e. 10 Gbps when it is stationary and 9.2 Gbps when there are environmental changes (user or object movement in the room). The medium access control (MAC) protocol used to share the VLC medium between users should include a repetitive training period to perform the CS and the beam delay adaptation technique. The design of the MAC protocol is not considered in this work. Our delay adaptation algorithm has been considered at one given receiver location in a single user scenario. In the case of a multiuser scenario, scheduling [51] can be used where the delay adaptation algorithm is chosen to maximise the 3 dB channel bandwidth and the SNR in a given region for a given time period. The delay adaptation can be implemented through array element delayed switching.

The photocurrents received in each branch can be amplified separately and can be processed using different methods such as selection combining (SC), equal gain combining (EGC) or maximum ratio combining (MRC) to maximise the power efficiency of the system. The MRC technique can achieve better performance compared to other methods [23], [52]. Therefore, the ADRR-LD system employs an MRC approach.

B. IMGR-LD

The IMGR-LD system has a similar room configuration and uses the same algorithms as the previous system (i.e. CS and delay adaptation). However, the main difference between the two systems is the type of receiver (see Fig.6b). An imaging receiver with 50 pixels is employed here. The IMGR-LD system combines the signals coming from eight relays by using the MRC method.

C. SBIMGR-LD

In contrast to IMGR-LD, in the SBIMGR-LD system only one relay sends the information to the receiver (i.e. the relay closest to the receiver) as shown in Fig.6c. The CS algorithm is used to find the optimum path between transmitter and relay. Then, a select-the-best (SB) algorithm is applied between relays and receiver to find the closest relay to the receiver. The SB algorithm identifies the closest relay to the receiver according to the following steps:

1- A pilot signal is sent from one of the relays.
2- SNR is estimated at the receiver by pixel 1 of the imaging receiver.
3- Repeat step 2 for other pixels in the imaging receiver.
4- Repeat steps 2 and 3 for other relay units.
5- The receiver sends (using VLC or an infrared beam) a low data rate control feedback signal to inform the controller of the SNRs associated with each relay.
6- The relay that yields the best SNR is chosen by the controller (typically the closest relay to the receiver in our simulations).
7- The controller activates a silent mode for the remaining six relays and keeps the closest relay to the transmitter 'ON' to receive information signals from the transmitter, and it also keeps the closest relay to the receiver 'ON' for transmission (see Fig.6c). When the transmitter and receiver are at the same position (special case) only one relay will be 'ON' to receive and transmit information signals.

Like IMGR-LD, SBIMGR-LD employs a delay adaptation technique to improve SNR (note SNR includes eye opening, see equation (5) in [53]). The time taken by our algorithms (i.e. CS, SB and delay adaptation) is equal to 25 ms (8 relays × 1 ms (for CS) + 8 relays × 1 ms (for SB) + 9 RGB-LDs in each relay unit × 1 relay unit × 1 ms (for delay adaptation)). Therefore, 100% of the specified data rate can be achieved by the adaptive system when it is stationary and 97.5% in the case of transmitter or receiver movement. The proposed algorithms (BS, CS and DAT) require a repetitive training and feedback channel from the receiver to the controller at a low data rate.

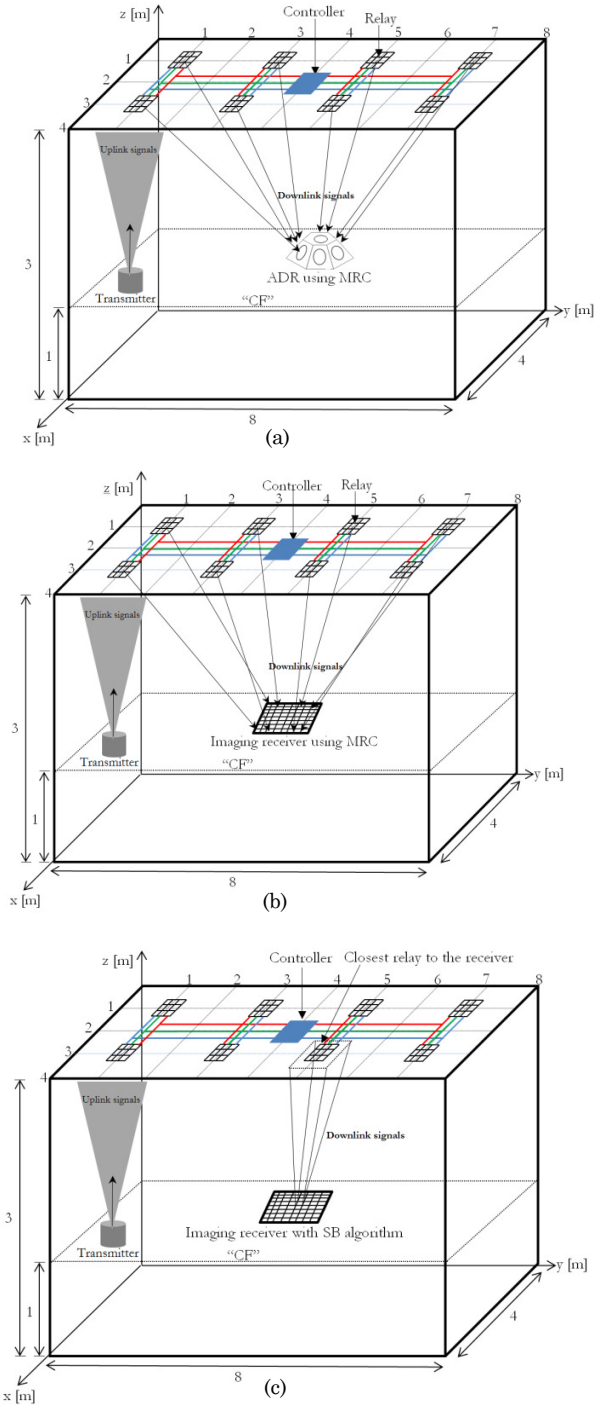

Fig.6: Systems configurations (a) ADRR-LD system, (b) IMGR-LD system and (c) SBIMGR-LD system.

An IR diffuse channel is suggested to achieve this, while the transmitter uses the VLC channel to send the data to the relay unit. Fig.7 shows a block diagram of the transmitter, relay and receiver with uplink and downlink channels (note that if a VLC transmitter near the user (laptop for example) is deemed too bright for user comfort, an IR uplink can be implemented). After CS the VLC transmitter sends the information signals, the relay unit receives the data and then the controller (a Microchips 32 bits microcontroller was used as the controller (PIC32MX110F016B) [54]) broadcasts the information to all relays. The backbone of our room network is for example based on plastic optical fibre (POF) cables (multimode fibres or even single mode fibres can be used to support higher data rates in future) and there are used for illumination (LDs light engine is used to generate RGB lasers) and to carry the data. RGB LDs emit the same information signal simultaneously. The use of a RGB triplet in such devices could potentially deliver data rates in the order of 30 Gbps by using WDM. It should be noted that the source of the information (transmitter) is fixed and located on the CF, its main function is to send the information signals to relays. Each mobile user has a compact transceiver that has the ability to send and receive data. The size of the photo detector and concentrator are acceptable in mobile terminals and they can be securely fixed to the mobile unit.

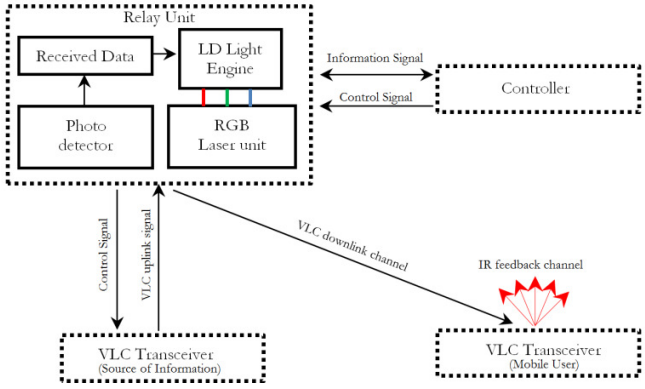

Fig.7: Block diagram of the relay assisted VLC system.

VI. Simulation Results and Discussion

We evaluated the performance of the proposed systems (ADRR-LD, IMGR-LD and SBIMGR-LD) using ADR and imaging receivers in an empty room in the presence of multipath dispersion and mobility. The proposed systems are examined in fourteen different locations when the receivers move along the *y*-axis and the transmitter is at the room centre (worst case scenario). The results are presented in terms of impulse response, delay spread, 3 dB channel bandwidth and SNR. Due to the symmetry of the room, the results for x=3m equal the results for x=1m, therefore only x=1m and x=2m results are shown along the *y*-axis.

A. *Impulse Responses*

The impulse responses of the ADRR-LD, IMGR-LD and SBIMGR-LD at the room centre are depicted in Fig.8 (a), (b) and (c), respectively. It can be seen that the SBIMGR-LD impulse response is better than that of ADRR-LD and IMGR-LD systems. The impulse responses of the three systems consist of first and second reflection components as well as LOS.

It can be noted that received power from reflection components in the SBIMGR-LD system has lower power than in ADRR-LD or IMGR-LD. This is because only the closest relay to the receiver transmits the information signals, whereas in the case of the ADRR-LD and IMGR-LD systems, eight relays emit optical signals together.

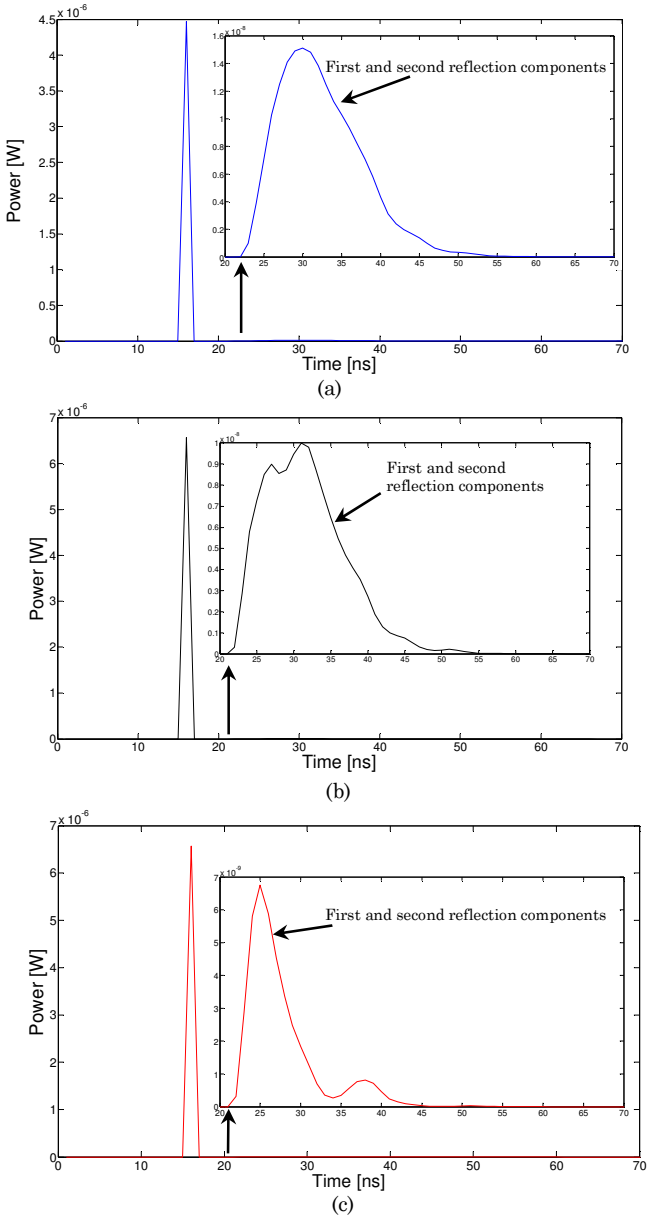

Fig.8: Impulse responses at room centre (x=2m, y=4m, z=1m) (a) ADRR-LD, (b) IMGR-LD and (c) SBIMGR-LD.

B. *Delay Spread*

Fig.9 presents the delay spread of the proposed systems when receivers move at x=1m and x=2m along the y-axis (in 1 m step). A 0.2 m user step has been considered and combined with the results of the 1 m step as shown in Figs. 9, 10 and 11. Reducing the step size from 1 m to 0.2 m led to smoothing the results curves for the delay spread, 3 dB channel bandwidth and SNR. The results show that the SBIMGR-LD has the lowest delay spread compared with ADRR-LD and IMGR-LD. This is attributed to two reasons: first, in SBIMGR-LD only one relay sends information signals towards the receiver. Second, LOS is dominant over other components. The results indicate that employing the SBIMGR-LD system instead of the ADRR-LD system can reduce the delay spread by a factor of 1.6, from 0.01 ns to 0.006 ns in the worst communication path. It was observed that, at x=1m in the ADRR-LD and the IMGRR-LD systems, the delay spread can be lower than at x=2m. This is due to link distances which increase at x=2m leading to increase in delay spread. However, the SBIMGR-LD system delay spread is about the same in both lines x=1m and x=2m.

C. *3 dB Channel Bandwidth*

Although the transmitter modulation bandwidth problem in the traditional VLC system can be tackled by replacing LEDs with LDs, channel bandwidth remains an issue that needs to be solved to achieve multi-gigabit data rates. Previous work has shown that adopting LDs with an imaging receiver can provide a 3 dB channel bandwidth of more than 4 GHz [23]. The 3 dB channel bandwidth achieved by three systems at x=1m and x=2m is depicted in Fig.10. The results show that the SBIMGR-LD system offers 3 dB channel bandwidth of more than 26 GHz in the worst case. The minimum communication channel bandwidth of the ADRR-LD system was 8.3 GHz at x=2m. The significant increase in the channel bandwidth enables our proposed systems to operate at higher data rates using a simple modulation technique, OOK [55]. Personick's analysis shows that the optimum receiver bandwidth is 0.7 times the bit rate [56]. For example, a 10 Gbps data rate requires a 7 GHz overall (channel and system chain) bandwidth. To the best of our knowledge, this is the highest channel bandwidth and data rates reported for an indoor mobile VLC system with simple modulation format (i.e. OOK). Also, it should be noted that the results in Fig.10 are in agreement with the general observation made in Fig.9. For instance, in the SBIMGR-LD system at the point x=1m and y=2m, the delay spread is the lowest resulting in the highest channel bandwidth (see Fig.10 (a)). Similar agreement is observed when comparing other locations.

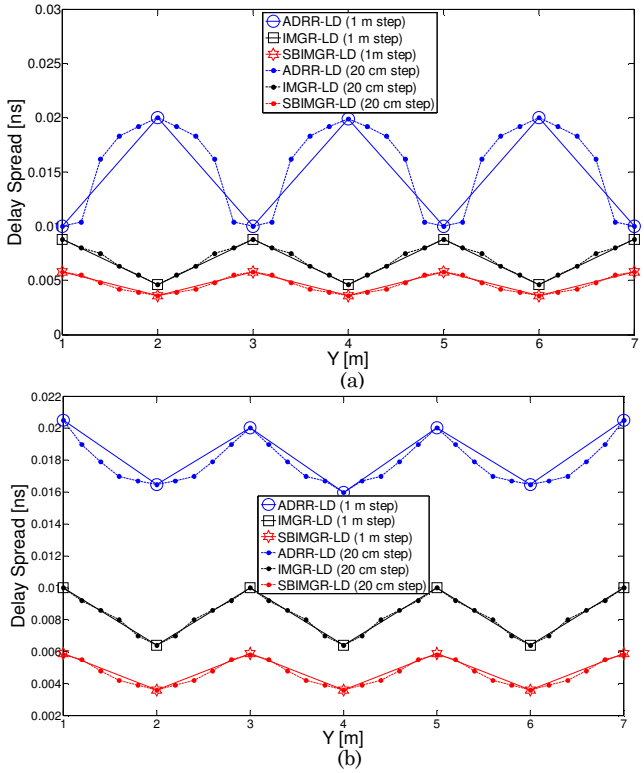

Fig.9: Delay spread of the three systems, (a) at x=1m and (b) at x=2m and along y-axis.

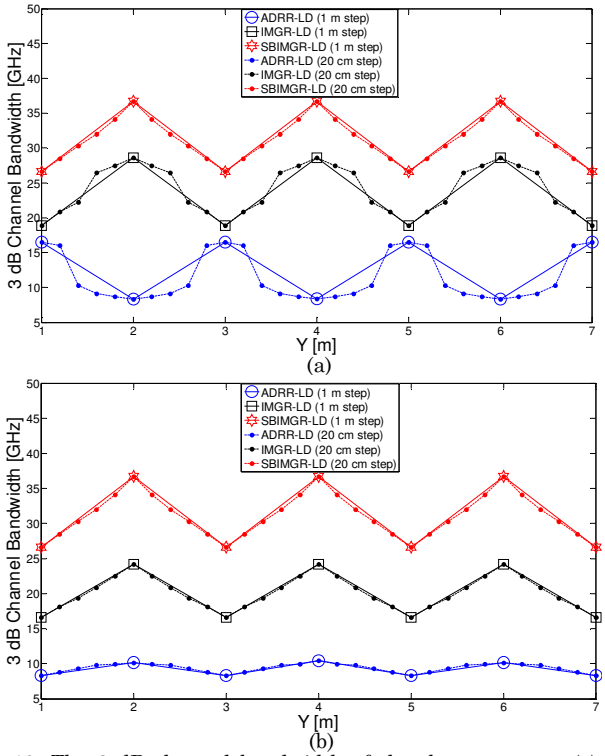

Fig.10: The 3 dB channel bandwidth of the three systems, (a) at x=1m and (b) x=2m and along y-axis.

Third order reflections were also considered when the receiver was located at the worst case scenario position (2m, 4m, 1m). Table II shows the delay spread and 3 dB channel bandwidth of the proposed systems with and without third order reflections. The increase in the delay spread and reduction in receiver bandwidth were extremely small when the third order reflections were included. This can be attributed to strong LOS components and the limited range of the rays accepted by the small FOV branches of the ADR and pixels in the imaging receiver with narrow FOV. This is an important distinction between VLC systems and IR-OW systems, where, in the latter, third order reflections may play a significant role at high data rates [25]. Received power from the third order reflections for the three systems was extremely low compared to LOS, first order and second order reflections. For example, in the IMGR-LD system, the LOS, first order, second order and third order received powers were 6.36 μW, 0.2 μW, 0.131 μW and 0.01 μW respectively, which means that the third order reflections have a power contribution of about 0.14% of the total power received. Therefore, for convenience, computer analysis up to second order reflections has been considered in this study.

TABLE II
DELAY SPREAD AND 3 dB CHANNEL BANDWIDTH WITH AND WITHOUT 3rd ORDER REFLECTIONS

Receiver at (2m, 4m, 1m)	ADRR	IMGR	SBIMGR
Delay spread [ns] up to 2nd order reflections	0.0159	0.0064	0.0036
Delay spread [ns] up to 3rd order reflections	0.0162	0.0066	0.0037
3 dB Channel bandwidth [GHz] up to 2nd order reflections	10.42	24.2	36.7
3 dB Channel bandwidth [GHz] up to 3rd order reflections	10.28	23.5	36.2

D. SNR Analysis

Indoor VLC communication systems are strongly impaired by ISI and mobility. The conventional OOK-BER of the indoor VLC system can be given as [45]:

$$BER = \frac{1}{2}\, erfc\left(\sqrt{SNR/2}\right) \tag{16}$$

where $erfc$ is the complementary error function. In this paper, we consider the MRC method for processing the electrical signals from different branches in the ADR and pixels in the imaging receiver. The MRC approach utilises all branches and pixels. The output signals of all the branches or pixels are combined through an adder circuit. Each input to the circuit is added with a weight proportional to its SNR to maximise the SNR. The SNR_{MRC} is given by [45]:

$$SNR_{MRC} = \left(\frac{\left(\sum_{i=1}^{j} R(P_{s1i}-P_{s0i})W_i\right)^2}{\sum_{i=1}^{j} {\sigma_t}^2 {W_i}^2}\right) \tag{17}$$

where j = 50 when our imaging receiver is used and j = 7 in the case of our ADR, R is the receiver responsivity (0.4 A/W) and P_{s1} and P_{s0} are the powers associated with logic 1 and 0, respectively. ${\sigma_t}^2$ is the variance of the total noise which is the sum of shot noise, thermal noise and shot noise associated with the received signal. σ_t can be calculated as [45]:

$$\sigma_t = \sqrt{\sigma_{shot}^2 + \sigma_{preamplifier}^2 + \sigma_{signal}^2} \tag{18}$$

where σ_{shot}^2 represents the background shot noise component, $\sigma_{preamplifier}^2$ represents the preamplifier noise component and σ_{signal}^2 represents the shot noise associated with the received signal. In this paper, for a bit rate of 10 Gbps, we used the p-i-n FET trans-impedance preamplifier as in [57]. W_i is the weight of each pixel $\left(\frac{R(P_{s1}-P_{s0})}{{\sigma_t}^2}\right)$. Then the SNR_{MRC} can be written as [45]:

$$SNR_{MRC} = \left(\frac{\left(\sum_{i=1}^{j} R(P_{s1i}-P_{s0i})\left(\frac{R(P_{s1}-P_{s0})}{{\sigma_t}^2}\right)\right)^2}{\sum_{i=1}^{j} {\sigma_t}^2 \left(\frac{R(P_{s1}-P_{s0})}{{\sigma_t}^2}\right)^2}\right)$$

$$= \sum_{i=1}^{j} \frac{\left(R^2 (P_{s1i}-P_{s0i})^2\right)}{{\sigma_t}^2} = \sum_{i}^{j} SNR_i \tag{19}$$

To evaluate the performance of ADRR-LD, IMGR-LD and SBIMGR-LD at high bit rates, the SNR was calculated at 10 Gbps. Fig.11 shows the SNR_{MRC} of three mobile VLC systems operating at 10 Gbps. The IMGR-LD and the SBIMGR-LD systems outperform the ADRR-LD system. The imaging receiver produced significant improvements in SNR compared to the ADR. This is attributed to reducing the contribution of the reflection component by using narrow FOV pixels and by appropriately weighing (MRC-fashion) the pixels' contributions resulting in an emphasis on the direct power component (i.e. LOS).

SBIMGR-LD has lower SNRs values at x=1m and x=2m compared with the IMGR-LD system. This is due to only

one source of information transmitting data (one relay transmits information), whereas in IMGR-LD eight relays emit information signals simultaneously and, at the receiver side, MRC is used which leads to significant improvement in SNR.

Simulation results at x=1m showed that the IMGR-LD system achieved about 15.7 dB SNR when using the MRC approach. This means that the *BER* provided by our IMGR-LD system is better than 10^{-9} at 10 Gbps. However, the SNR is observed to decay slightly when the receiver moved along the x=2m (*BER* better than 10^{-7}). This decay occurs due to the increased distance between relay and receiver. Forward error correction coding (FEC) can be used to reduce further the *BER* from 10^{-7} to 10^{-9} in this proposed IMGR-LD system.

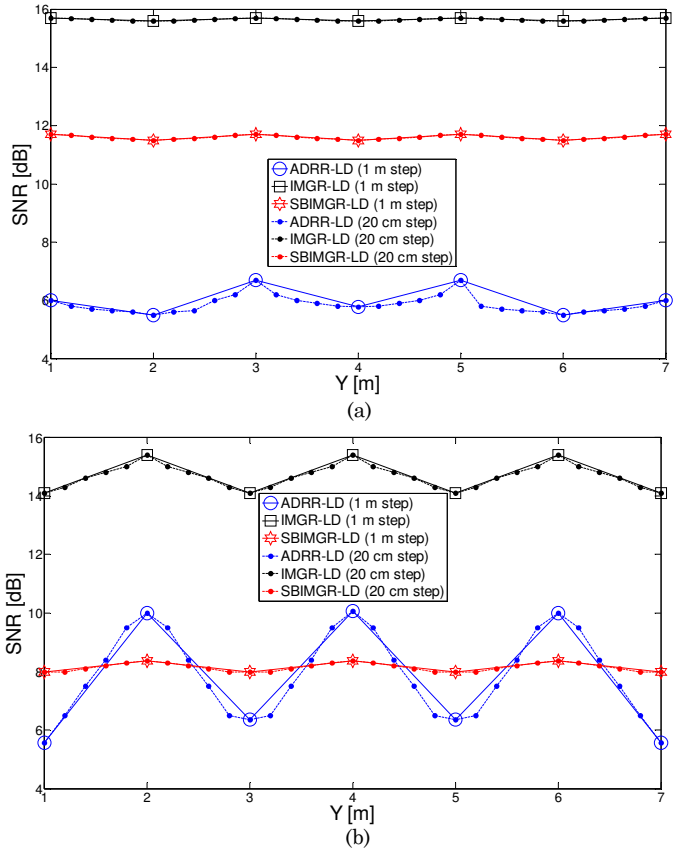

Fig.11: SNR of ADRR-LD, IMGR-LD and SBIMGR-LD systems when operated at 10 Gbps (a) at x=1m and (b) at x=2m and along y-axis.

Tables (III), (IV) and (V) present the *BER* at 10 Gbps of the ADRR-LD, IMGR-LD and SBIMGR-LD, respectively. Due to room symmetry, we calculated *BER* for 1 m to 4 m along the y-axis. If we compare the values in Tables III, IV and V for x=1m and x=2m, we can clearly see that the IMGR-LD system has the best performance compared to the other systems. At x=2m, the *BER* of the IMGR-LD system has increased slightly. However, this increase does not severely affect the performance of the system; for example, the smallest value of *BER* in Table IV at x=2m is equal to 2.9×10^{-7}, and this value can provide a strong communication link.

TABLE III BER PERFORMANCE OF THE ADRR-LD SYSTEM

x = 1m				
Receiver Location y-axis	1m	2m	3m	4m
BER	2.8×10^{-2}	3.6×10^{-2}	1.4×10^{-2}	3×10^{-2}
x = 2m				
Receiver Location y-axis	1m	2m	3m	4m
BER	2.9×10^{-2}	7.2×10^{-4}	2.3×10^{-2}	7.2×10^{-4}

TABLE IV BER PERFORMANCE OF THE IMGR-LD SYSTEM

x = 1m				
Receiver Location y-axis	1m	2m	3m	4m
BER	5.6×10^{-10}	8.6×10^{-10}	5.6×10^{-10}	8.6×10^{-10}
x = 2m				
Receiver Location y-axis	1m	2m	3m	4m
BER	2.9×10^{-7}	3.3×10^{-9}	2.9×10^{-7}	3.3×10^{-9}

TABLE V BER PERFORMANCE OF THE SBIMGR-LD SYSTEM

x = 1m				
Receiver Location y-axis	1m	2m	3m	4m
BER	7.2×10^{-5}	9.2×10^{-5}	7.2×10^{-5}	9.2×10^{-5}
x = 2m				
Receiver Location y-axis	1m	2m	3m	4m
BER	6.2×10^{-3}	4.6×10^{-3}	6.2×10^{-3}	4.6×10^{-3}

In Fig.12, the SNR penalty was calculated based on the old CS and old DAT settings while in motion. The results show the SNR penalty incurred as a result of mobility. The proposed systems' design should allow a link margin. For instance, with a link power margin of 3 dB for ADRR-LD, Fig.12 shows that adaptation has to be done every time the receiver moves by 0.6 m approximately. If the SNR penalty is lower than 1 dB, as desired in ADRR-LD, then Fig.12 shows how often the system has to adapt its settings. For example, for the SNR penalty to be below 1 dB, the system has to adapt the CS and delay adaptation every 0.2 m approximately, which corresponds to a 0.2 second adaptation frequency. It should be noted that this adaptation has been done at the rate at which the environment changes and not at the system's bit rate. In addition, we can clearly see that the IMGR-LD and SBIMGR-LD systems outperform the ADRR-LD and this is due to using the imaging receiver instead of the ADR.

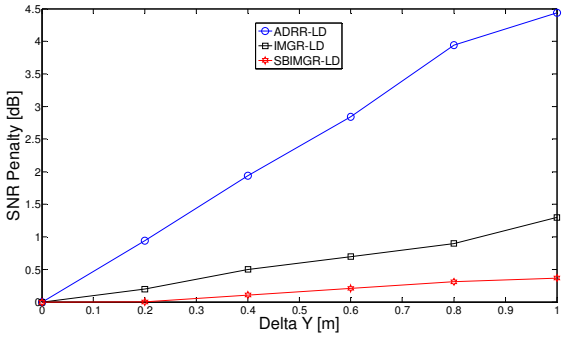

Fig.12. The SNR penalty of the proposed systems when the receiver moves from the optimum location at (2m, 1m, 1m) along y axis.

VII. Small Office Environment

A simulation tool was developed to model a new VLC room with dimensions of 5×5×3 m3 to enable comparison with previous work [2], [58] (room dimensions, source distribution, surrounding surface reflectance and receiver positions are similar to [2]), and to evaluate the performance of the proposed systems in two different room sizes. The results are presented in terms of delay spread and SNR, and compared to the results presented in the previous Section. Fig.13 shows the new VLC room (small office).

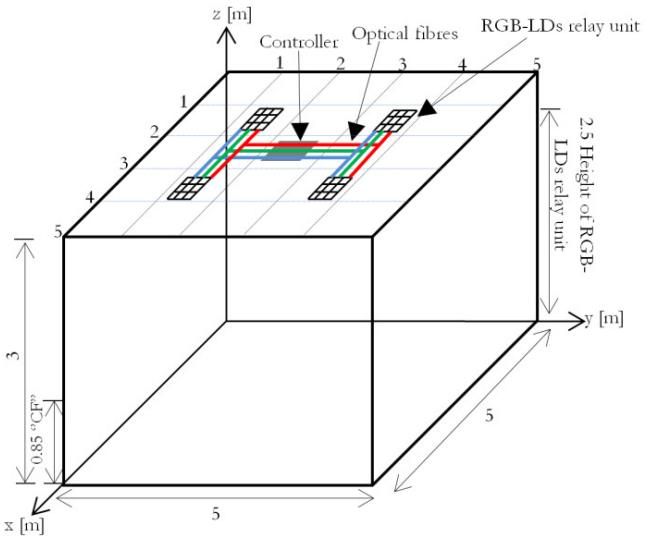

Fig.13: VLC system room with dimensions of 5×5×3 m³.

A. Delay Spread

Fig.14 presents the delay spread of the proposed systems when receivers were moved at x=1.25m (line underneath relay units) and x=2.5m (middle of the room) along the y-axis. It should be noted that the delay spread of the proposed systems in the small office (5×5×3 m³) is much lower than that in the large office (4×8×3 m³), and this could be due to two reasons: 1) the distance between the relay unit and receiver is less than that in the large office and 2) decreasing the room size leads to a decrease in the number of reflectance elements which decreases the power received from the reflections. The delay spread results are comparable to the results in [58]. However, in the current work the delay spread becomes very low because we used an imaging receiver and ADR with narrow FOV, which lead to a reduction in the effect of the reflection components. Due to the symmetry of the room, the results for x=1.25m, y=1 are equal to the results for x=1.25m, y=4 (or y=2 and y=3); a similar behaviour was observed when the receiver moved along the x=2.5m line.

B. SNR

Fig.15 illustrates the SNR of the proposed systems at high data rates (10 Gbps) in the small office. It was observed that the SNR of the three systems in the small room was higher than that in the large room due to the small distance between the transmitter and receiver, which lead to a reduced path loss and increased SNR. It should be noted that the IMGR-LD system outperformed the other systems (ADRR-LD and SBIMGR-LD) in the small office (5×5×3 m³), as it did in the large office (4×8×3 m³).

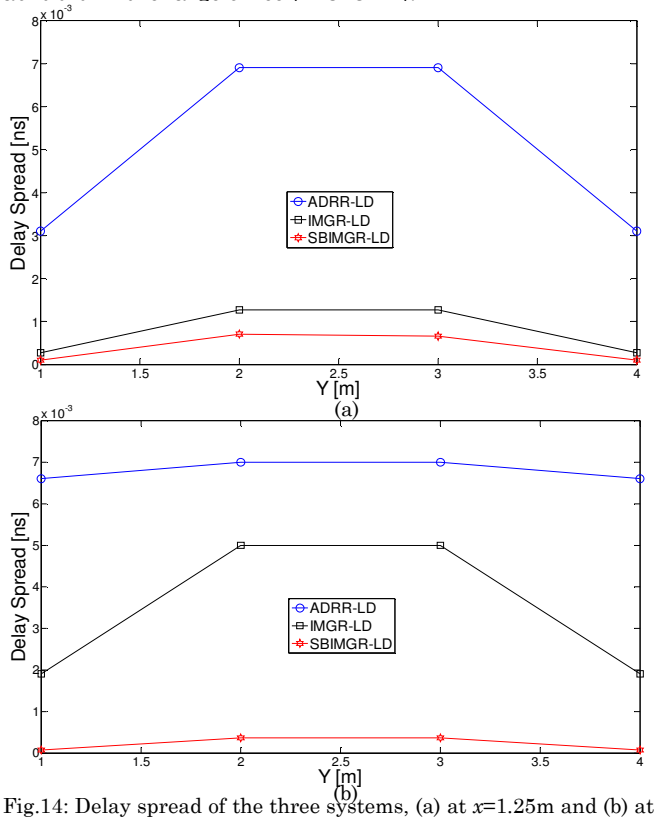

Fig.14: Delay spread of the three systems, (a) at x=1.25m and (b) at x=2.5m and along y-axis.

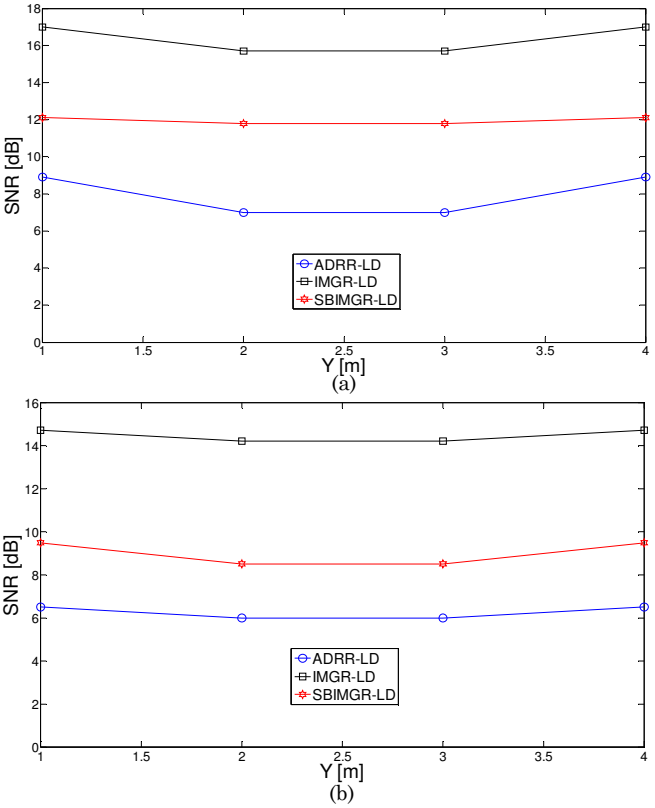

Fig.15: SNR of the three systems, (a) at x=1.25m and (b) at x=2.5m and along y-axis.

VIII. Robustness to Shadowing and Signal Blockage

Shadowing, signal blockage and mobility are among the main impairments that impact the performance of VLC systems in indoor environments. Therefore, we extended the analysis and evaluation of the performance of the proposed systems to a harsh indoor environment with mobility. The simulation was conducted in a room that was comparable in dimensions to that explained in Section III (see Fig.2). Fig.16 illustrates a realistic room environment where a door, windows, cubicle partitions, bookshelves and furniture are all present. The ceiling and the walls that surround the windows have diffuse reflectivity of 0.8. The door is considered to not reflect any signal, therefore its diffuse reflectivity is set to zero. Glass windows were assumed to not reflect any signal, therefore their reflectivity was set to 0 for the three glass windows (i.e. all the rays that reach the windows pass through and are not reflected). Thus we consider a worst case scenario where all rays pass through the glass windows instead of being reflected to the receiver side. Two of the walls: x=4m (excluding the door) and y=8m were covered by filling cabinets and bookshelves with a diffuse reflectivity of 0.4. It was assumed that signals that encountered a physical barrier were either blocked or absorbed. Additionally, desks, tables and chairs inside the realistic room have similar reflectivities to the floor (i.e. 0.3). The complexity of the environment in this room results in shadowing created by low reflectivity objects and physical partitions. Comparisons were performed between the proposed systems in two different environments (i.e. room A that is an empty room and room B that is a realistic room) with all systems operating at 10 Gbps with full mobility. In Section III a simulation package based on a ray-tracing algorithm was developed using MATLAB to compute the impulse response of the different VLC systems in an empty room. In this section, additional features were introduced for a realistic room. In the realistic environment for each receiver location, the first step is to check the availability of the LOS component (certain conditions were introduced to the simulator to check the existence of LOS, first and second order reflection components in each location) and then the received power due to first and second order reflections is calculated. In some locations over the CF some of the LOS components were blocked by mini cubicles, and this affected the SNR severely. Fig.17 shows a block diagram of the simulator with ADR and imaging receiver.

Channel impulse responses at the room centre (i.e. x=2m and y=4m, chosen as they represent the worst communication link over the entire CF (motion between cubicles)) for the ADRR-LD, IMGR-LD and SBIMGR-LD systems are shown in Fig.18 for rooms A and B. It should be noted that the impulse responses of the proposed systems were dominated by short initial impulses due to the LOS paths between the transmitters and receiver. In addition, it can be clearly seen that the IMGR-LD and SBIMGR-LD systems have good robustness against shadowing and mobility, and they have the ability to maintain LOS even in this harsh environment (i.e. room B), which is attributed to the number of transmitters that are distributed on the ceiling (i.e. eight RGB LD light units). However, the amount of received optical power from the reflections in room B was less than that received in room A, as shown in Fig.18, and this was due to the existence of the door, windows, cubicles, partitions and bookshelves in room B that lead to reduced multipath propagation. Although the received power from the reflections was severely affected in room B, the LOS component remained the same in both room configurations in both systems, and the LOS component had the largest impact on the system performance.

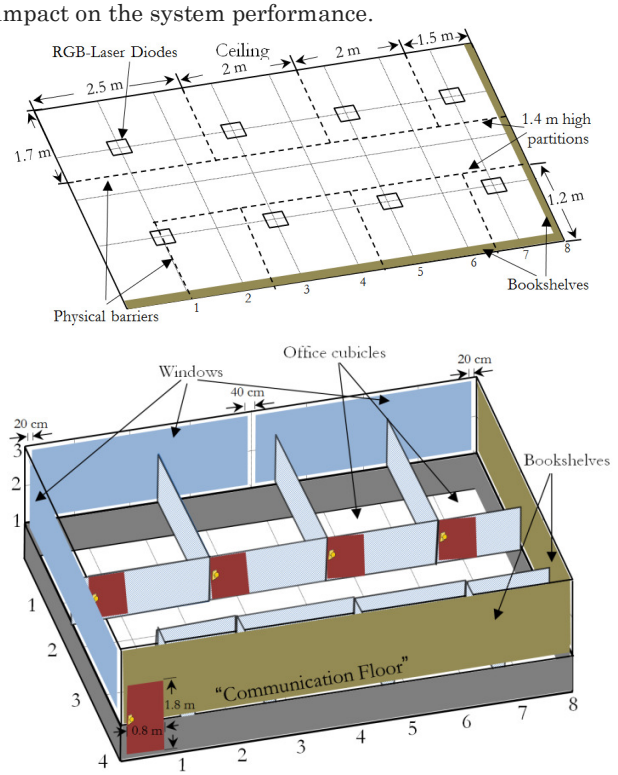

Fig.16: Realistic room with a number of rectangular-shaped cubicles with surfaces parallel to the room walls, a door, three large glass windows and furniture, such as bookshelves and chairs.

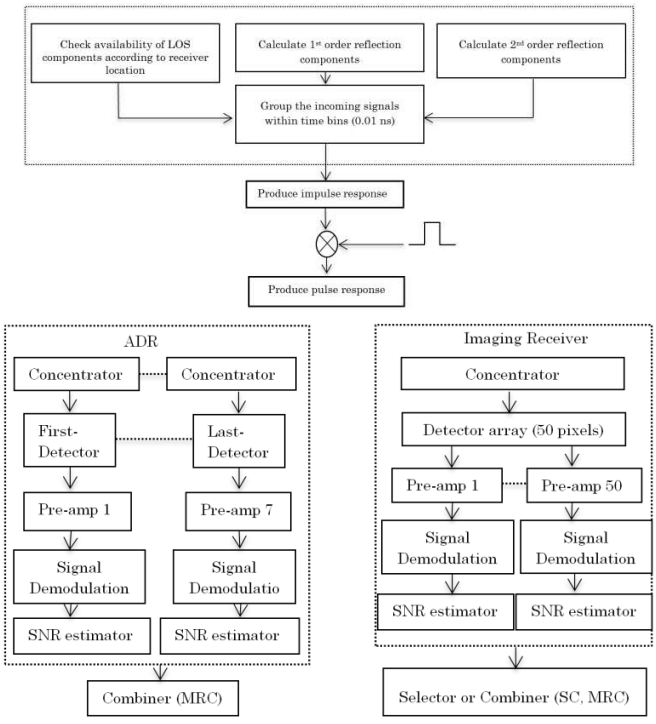

Fig.17: Block diagram of the simulator.

For example, the received optical power associated with the IMGR-LD system in room A was 6.69 μW, whereas it was 6.63 μW in room B, which indicates that the reduction in power was negligible (the reduction in power was 0.063 μW). Moreover, it can be noted that the effect of shadowing on the ADRR-LD system was clear when the receiver was located at the room centre in room B. The LOS received power in room A was 4.5 μW, whereas it was 2.25 μW in room B (about 3 dB reduction in received power), and this was due to one of the LOS components being blocked by the wall of a cubicle. These impulse responses suggest that the ADRR-LD system performs better in room A (without shadowing) than in room B, and the IMGR-LD and SBIMGR-LD systems were affected by the shadowing geometry considered (office cubicles).

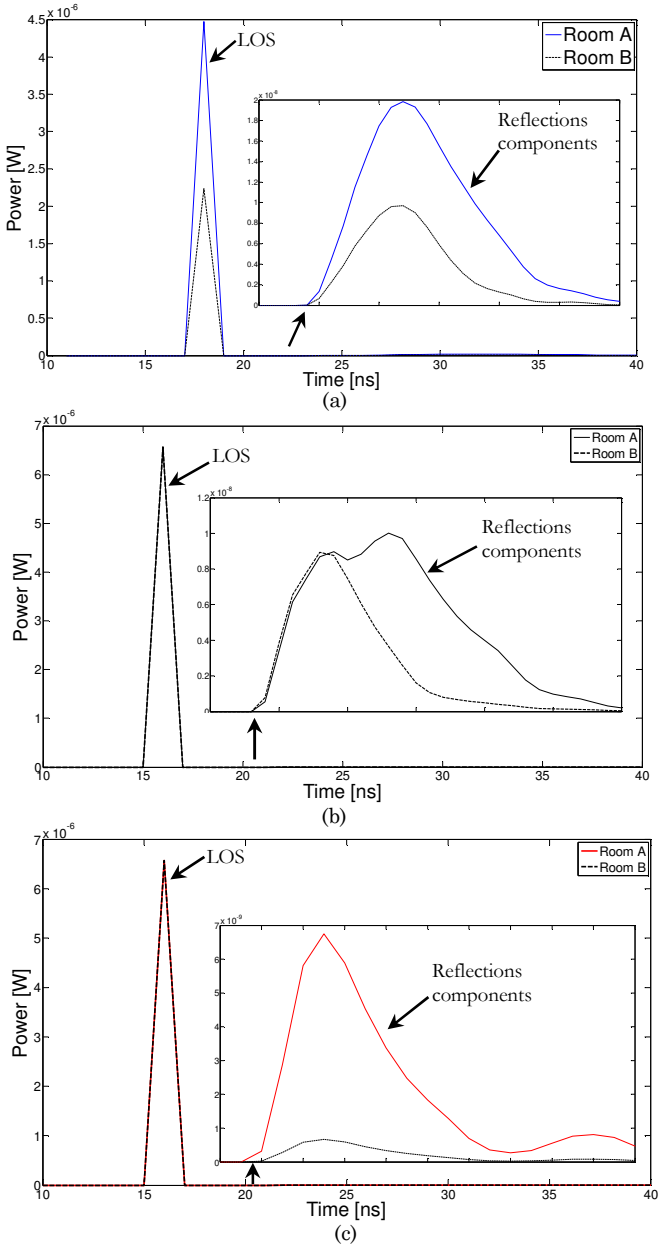

Fig.18: Impulse responses at room centre (x=2m, y=4m, z=1m) in two different environments (rooms A and B) (a) ADRR-LD, (b) IMGR-LD and (c) SBIMGR-LD.

Fig.19 shows the SNR results against receiver location for the proposed systems in the two room scenarios. It is observed that the performance of the IMGR-LD and SBIMGR-LD systems are comparable in rooms A and B, and this can be attributed to the LOS links available in the entire CF, which protects against shadowing and mobility in these systems. It can be noticed that the ADRR-LD system has lower SNR in room B than in room A (3 dB SNR reduction approximately). This is because, when the ADR moves along lines x=1m and x=2m, some transmitters (RGB-LD relay unit) cannot be detected by receivers due to cubicles.

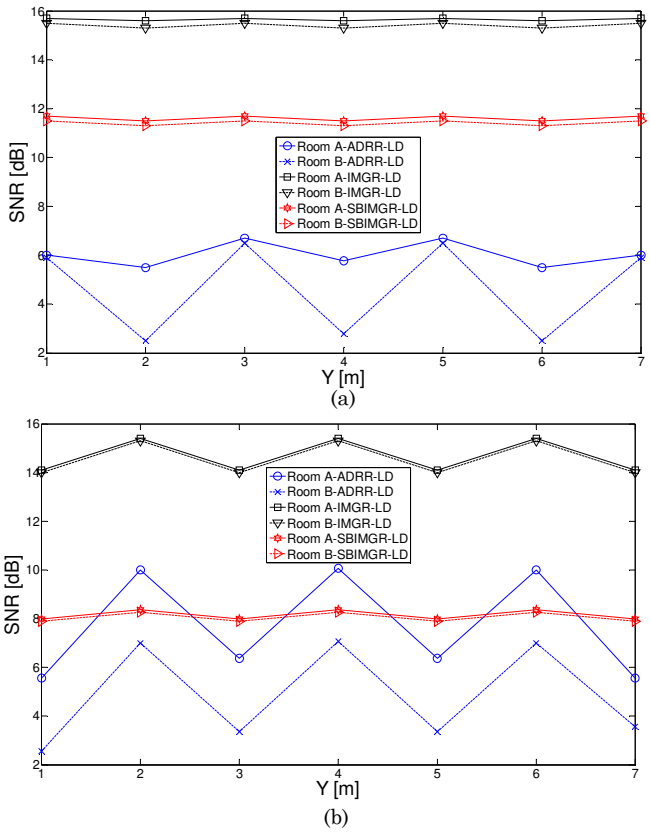

Fig.19: SNR of ADRR-LD, IMGR-LD and SBIMGR-LD systems in two different environments (rooms A and B) when the systems operated at 10 Gbps at (a) x=1m and (b) x=2m and along the y-axis.

The proposed systems are able to achieve a very high channel bandwidth (8.3 GHz and beyond, see Fig.10), which is more than enough to operate at 10 Gbps. In addition, the backbone of the room network is fibre cable that is able to carry 10 Gbps, and the modulation bandwidth of the LDs (the sources used in our work) can be in the GHz range (off-the-shelf LDs). Furthermore, the photo detector (PD) area that was used in our work (imaging receiver and ADR) was very small (4 mm2) to ensure that the internal capacitance of the PD would not affect the performance of our receivers. The fabrication and testing of a high speed VLC receiver array are very challenging tasks. To the best of our knowledge, there is no commercial high speed VLC receiver to date that has specially been designed for indoor VLC use. At a data rate of 10 Gbps, most of the components will probably be adopted from the IR-OW and optical fibre domain [59], which is not ideal for VLC.

IX. Conclusions

In this paper, we proposed, designed and investigated the concept of relays in a VLC system. We introduced two novel algorithms (CS and SB) to create optimum transmitter-relay and relay-receiver communication links.

Three novel VLC systems (ADRR-LD, IMGR-LD and SBIMGR-LD) are introduced. These VLC systems use LDs instead of LEDs as transmitters, and they use two different types of receiver: an ADR with 7 branches and an imaging receiver with 50 pixels.

We optimised the FOVs, AZs and ELs of the ADR and the FOVs of the imaging receiver.

In the worst case scenario, SBIMGR-LD achieves significant improvements in VLC channel bandwidth and delay spread over the ADRR-LD and IMGR-LD systems. It has the ability to achieve 26 GHz channel bandwidth (about 0.0058 ns delay spread). On the other hand, the IMGR-LD outperforms the ADRR-LD and the SBIMGR-LD systems in SNR (14.1 dB in the worst case scenario). The *BER* provided by our IMGR-LD system is better than 10^{-7} at 10 Gbps in the worst case scenario.

Different room sizes were also considered to examine the performance of the proposed systems. The performance of the proposed systems was better in the small office than the large office and this is due to the distance between the transmitter and receiver, which was smaller and led to reduced path loss, delay spread and increased SNR.

The proposed systems were evaluated under diverse situations including an empty room and a room with very strong shadowing effects resulting from mini cubicle offices. The IMGR-LD and SBIMGR-LD systems have good robustness against shadowing and mobility, and they have the ability to maintain LOS even in this harsh environment. But the ADRR-LD system performance was severely affected when it is operated in the realistic environment characterized by shadowing.

To the best of our knowledge, the data rates achieved by our proposed systems (i.e. 10 Gbps) are the highest data rates for an indoor mobile VLC system with simple modulation (OOK) to date.

Future work will address methods to enhance the SNR of the IMGR-LD system to achieve data rates higher than 10 Gbps.

Acknowledgment

Ahmed Taha Hussein would like to acknowledge with thanks the Higher Committee for Education Developments in Iraq (HCED) and the University of Mosul for financial support during his research.

References

[1] F. R. Gfeller and U. H. Bapst, "*Wireless in-house data communication via diffuse infrared radiation*," Proc. IEEE, vol. 67, no.11, pp.1474-1486, 1979.

[2] T. Komine and M. Nakagawa, "*Fundamental analysis for visible-light communication system using LED lights*," IEEE Transactions on Consumer Electronics, vol.50, no.1, pp.100-107, 2004.

[3] A. T. Hussein and J. M. H. Elmirghani, "*A Survey of Optical and Terahertz (THz) Wireless Communication Systems*," IEEE Communications Surveys & Tutorials, (to be submitted), 2015.

[4] H. L. Minh, D. C. O Brien , G. Faulkner , L. Zeng , K. Lee , D. Jung and Y. Oh, "*80 Mbit/s visible light communications using pre-equalized white LED*," in Proc. 34th European Conference on Optical Communication (ECOC), pp.1-2, 2008.

[5] A. M. Khalid, G. Cossu, R. Corsini, P. Choudhury, E. Ciaramella, "*1-Gb/s transmission over a phosphorescent white LED by using rateadaptive discrete multitone modulation*," IEEE Photonics Journal, vol.4, issue 5, pp.1465-1473, 2012.

[6] Z. Xie, K. Cui, H. Zhang, and Z. Xu, "*Capacity of MIMO visible light communication channels*," In Photonics Society Summer Topical Meeting Series, pp.159-160, 2012.

[7] C. Kottke, J. Hilt, K. Habel, J. Vučić, and K. Langer, "*1.25 Gbit/s visible light WDM link based on DMT modulation of a single RGB LED luminary*," In European Conference and Exhibition on Optical Communication, Optical Society of America, vol.3, no.66, pp.1-3, 2012.

[8] P. Butala, H. Elgala and T. Little, "*SVD-VLC: A novel capacity maximizing VLC MIMO system architecture under illumination constraints*,"Globecom Workshop on Optical Wireless Communications (OWC), 2013.

[9] M. Biagi, A. M. Vegni, S. Pergoloni,P. Butala and T. Little, "*Trace-orthogonal PPM - Space time block coding under rate constraints for visible light communication*," Journal of lightwave technology, vol.33, pp.481-494, 2015.

[10] S. Pergoloni, M. Biagi, S. Rinauro, S. Colonnese,R. Cusani,G. Scarano, "*Merging Color Shift Keying and Complementary Pulse Position Modulation for Visible Light Illumination and Communication*," IEEE Journal of Lightwave Technology, vol.33, no.1, pp.192-200, 2015.

[11]S. Zhang, S. Watson, J. McKendry, D. Massoubre, A. Cogman, R. K. Henderson, A. E. Kelly, and M. D. Dawson, "*1.5 Gbit/s multi-channel visible light communications using CMOS-controlled GaN-based LEDs*," Journal of Lightwave Technology, vol.31, no.8, pp.1211-1216, 2013.

[12] G. Cossu, A. M. Khalid, P. Choudhury, R. Corsini, and E. Ciaramella, "*3.4 Gbit/s visible optical wireless transmission based on RGB LED*," Optics express, vol.20, no.26, pp.501-506, 2012.

[13] D. Tsonev, H. Chun, S. Rajbhandari, J. McKendry, S. Videv, E. Gu, M. Haji, S. Watson, A. Kelly, G. Faulkner, M. Dawson, H. Haas, and D. O'Brien, "*A 3-Gb/s Single-LED OFDM-Based Wireless VLC Link Using a Gallium Nitride μLED*," IEEE Photon. Technol. Lett., vol. 26, no.7, pp.637–640, 2014.

[14] A. Neumann, J. J. Wierer, W. Davis, Y. Ohno, S. Brueck, and J. Y. Tsao. "*Four-color laser white illuminant demonstrating high color-rendering quality*," Optics express, vol.19, no.104, pp.982-990, 2011.

[15] D. S. Weber, A. Buck, and D. Christian Amann, "*Laser Light in the BMW i8 Design, System Integration and Test*," ATZ worldwide, vol.116, no.9, pp.44-49, 2014.

[16] K. A. Denault, M. Cantore, S. Nakamura, S. P. D. Baars, and R. Seshadri, "*Efficient and stable laser-driven white lighting*," AIP Advances, vol.3, no.7, pp. 2013.

[17] R. Gatdula, J. Murray, A. Heizler, and M. Shah, "*Solid State Lighting with Blue Laser Diodes*," [online] Available: *http://www.winlab.rutgers.edu/~crose/capstone12/entries/SolidStateLightingwBlueLaserDiodes-Revised.pdf*.Last access on 15/05/2015.

[18] C. Basu, M. Meinhardt-Wollweber, and B. Roth, "*Lighting with laser diodes*," Advanced Optical Technologies, vol.2, issue 4, pp.313-321, 2013.

[19] "LD Lighting Engine is a new type of light source from Toshiba," [online] Available: http://reefbuilders.com/2012/07/23/ld-lighting-engine-toshiba/. Last access on 15/05/2015.

[20] S. Soltic and A. Chalmers, "*Optimization of laser-based white light illuminants*," Optics express, vol.21, no.7, pp.8964-8971, 2013.

[21] J. Wierer, J.Y. Tsao and D.S. Sizov, "*Comparison between blue lasers and light-emitting diodes for future solid-state lighting*," Laser & Photonics Reviews, vol.7, no.6, pp.963-993, 2013.

[22] J. Gancarz, H. Elgala and T.D. Little, "*Impact of lighting requirements on VLC systems*," IEEE Communications Magazine, vol.51, no.12, pp.34-41, 2013.

[23] A. T. Hussein, and J.M.H. Elmirghani, "*Mobile Multi-gigabit Visible Light Communication System Employing Laser Diodes, Imaging Receivers and Delay Adaptation Technique in Realistic Indoor Environment*," IEEE Journal of Lightwave Technology, (accepted for publication), 2015.

[24] A. T. Hussein, and J.M.H. Elmirghani, "*High-Speed Indoor Visible Light Communication System Employing Laser Diodes and Angle Diversity Receivers*," International Conference on Transparent Optical Networks (ICTON), (accepted for publication), 2015.

[25] K. Lee, H. Park, and J.R. Barry, "*Indoor channel characteristics for visible light communications*," IEEE Communications Letters, vol.15, no.2, pp. 217-219, 2011.

[26] T. Komine, J. Lee, S. Haruyama and M. Nakagawa, "*Adaptive equalization system for visible light wireless communication utilizing multiple white LED lighting equipment*," IEEE Wireless Communications Transactions, vol.8, no.6, pp.2892-2900, 2009.

[27] J. Tan, K. Yang, and M. Xia, "*Adaptive equalization for high speed optical MIMO wireless communications using white LED*," Frontiers of Optoelectronics in China, vol.4, no.4, pp.454-461, 2011.

[28] H. Elgala, R. Mesleh, and H. Haas, "*Indoor broadcasting via white LEDs and OFDM*," IEEE Transactions on Consumer Electronics, vol.55, no.3, pp.1127-1134, 2009.

[29] Z. Wang, C. Yu, W. Zhong, J. Chen and W. Chen ,"*Performance of a novel LED lamp arrangement to reduce SNR fluctuation for multi-user visible light communication systems*," Optics Express, vol.20, no.4, pp.4564-4573, 2012.

[30] A. G. Al-Ghamdi, and J. M. H. Elmirghani, "*Optimization of a triangular PFDR antenna in a fully diffuse OW system influenced by background noise and multipath propagation.* Communications," IEEE Transactions on Communication, vol.51, no.12, pp.2103-2114, 2003.

[31] F. E. Alsaadi, and J. M. H. Elmirghani, "*Adaptive mobile line strip multibeam MC-CDMA optical wireless system employing imaging detection in a real indoor environment*," IEEE Journal of Selected Areas in Communications, vol.27, no.9, pp.1663–1675, 2009.

[32] T. J. Harrold, and A.R. Nix, "*Capacity enhancement using intelligent relaying for future personal communication systems*," IEEE in Vehicular Technology Conference, IEEE-VTS Fall VTC, vol.5, no.3, pp.2115-2120, 2000.

[33] J. N. Laneman, D. N. C. Tse, and G. W. Wornell, "*Cooperative diversity in wireless networks: efficient protocols and outage behavior*," IEEE Transactions Information Theory, vol. 50, no. 12, pp.3062–3080, 2004.

[34] E. C. van der Meulen, "*Three-terminal communication channels*," Advanced Appllication Probab., vol.3, no.1 pp.120–154, 1971.

[35] M. Safari and M. Uysal, "*Relay-assisted free-space optical communication*," IEEE Transactions on Wireless Communications, vol.7, no.12, pp.5441-5449, 2008.

[36] M. Karimi, and M. Nasiri-kenari, "*Free Space Optical Communications via Optical Amplify-and-Forward Relaying*," Journal of Lightwave Technology, vol.29, no.2, pp.242-248, 2011.

[37] G. Corbellini, "*Demo: LED-to-LED Visible Light Communication for Mobile Applications*," in Demo at ACM SIGGRAPH 2012, available at http://people.inf.ethz.ch/schmist/papers/Siggraph2012DemoVLC.pdf. Last access on 01/02/2015.

[38] F. E. Alsaadi, M. Nikkar and J. M. H. Elmirghani, "*Adaptive mobile optical wireless systems employing a beam clustering method, diversity detection, and relay nodes*," IEEE Transactions Communication, vol. 58, no.3, pp.869-879, 2010.

[39] "*European standard EN 12464-1: Lighting of indoor work places*," [online] Available:*http://www.etaplighting.com/uploadedFiles/Downloadable_documentation/documentatie/EN12464_E_OK.pdf*. Last access on 01/02/2015.

[40] I. Ashdown, and P. Eng, "*Photometry and radiometry*," President by Heart Consultants Limited, 2002.

[41] J. M. Kahn and J. R. Barry, "*Wireless infrared communications*," Proc. IEEE, vol.85, no.2, pp.265-298, 1997.

[42] A. Stimson, "*Photometry and radiometry for engineers*," New York, Wiley-Interscience, 1974.

[43] J. R. Barry, J. M. Kahn, W. J. Krause, E. A. Lee, and D. G. Messerschmitt, "*Simulation of multipath impulse response for indoor wireless optical channels*," IEEE Journal Selected Areas Communication, vol.11, no.3, pp.367-379, 1993.

[44] M. Biagi, T. Borogovac, and T.D.C. Little, "*Adaptive Receiver for Indoor Visible Light Communications*," Journal of Lightwave Technology, vol.31, no.23, p.3676-3686, 2013.

[45] A. G. Al-Ghamdi and J. M. H. Elmirghani, "*Line strip spot-diffusing transmitter configuration for optical wireless systems influenced by background noise and multipath dispersion*," IEEE Transactions Communication, vol.52, no.1, pp.37-45, 2004.

[46] A. G. Al-Ghamdi, and J. M. H. Elmirghani, "*Performance evaluation of a triangular pyramidal fly-eye diversity detector for optical wireless communications*," IEEE Communications Magazine, vol.41, no.3, pp.80-86, 2003.

[47] A. G. Al-Ghamdi, and J.M.H. Elmirghani, "*Characterization of mobile spot diffusing optical wireless systems with diversity receiver*," IEEE International Conference in Communications (ICC), 2004.

[48] F. E. Alsaadi, and J. M. H. Elmirghani, "*High-speed spot diffusing mobile optical wireless system employing beam angle and power adaptation and imaging receivers*," Journal of Lightwave Technology, vol.28, no.16, pp.2191–2206, 2010.

[49] P. Djahani, and J. M. Kahn, "*Analysis of Infrared Wireless Links Employing Multibeam Transmitter and Imaging Diversity Receivers*," IEEE Transactions Communication, vol.48, no.12, pp.2077-2088, 2000.

[50] *IEEE Standard for Local and Metropolitan Area Networks-Part 15.7: Short-Range Wireless Optical Communication Using Visible Light*, pp.1-309, 2011.

[51] P. Viswanath, D. N. C. Tse, and R. Laroia, "*Opportunistic beamforming using dumb antennas*," IEEE Transactions on Information Theory, vol.48, no.6 pp.1277-1294, 2002.

[52] A. G. Al-Ghamdi, and J.M.H. Elmirghani, "*Analysis of diffuse optical wireless channels employing spot-diffusing techniques, diversity receivers, and combining schemes*," IEEE Transactions on Communications, vol.52, no.10, pp.1622-1631, 2004.

[53] F. E. Alsaadi, M.A. Alhartomi, and J.M.H. Elmirghani, "*Fast and Efficient Adaptation Algorithms for Multi-Gigabit Wireless Infrared Systems*," Journal of Lightwave Technology, vol.31, no.23, pp.3735-3751, 2013.

[54]http://www.microchip.com/ParamChartSearch/chart.aspx?branchID=21 1&mid=10&lang=en&pageId=74. Last access on 15/05/2015.

[55] M. T. Alresheedi, and J.M.H. Elmirghani, "*10 Gb/s Indoor Optical Wireless Systems Employing Beam Delay, Power, and Angle Adaptation Methods With Imaging Detection*," Journal of Lightwave Technology, vol.30, no.12, pp.1843-1856, 2012.

[56] S. D. Personick, "*Receiver design for digital fiber optical communication system, Part I and II*," Bell System Technology Journal, vol.52, no.6, pp 843-886, 1973.

[57] E. M. Kimber, B. L. Patel, I. Hardcastle, and A. Hadjifotiou, "*High performance 10 Gbit/s pin-FET optical receiver*," Electronics Letters, vol.28, no.2, pp.120-122, 1992.

[58] T. Komine, "*Visible light wireless communications and its fundamental study*," (Doctoral dissertation, Ph. D. Dissertation- Nakagawa group). (Oline) Available at: http://iroha.scitech.lib.keio.ac.jp:8080/sigma/bitstream/handle/10721/2017/document.pdf?sequence=4. Last access on 15/05/2015.

[59] K. Wang, A. Nirmalathas, C. Lim, and E. Skafidas, "*High-speed indoor optical wireless communication system with single channel imaging receiver*," Optics express, vol.20, no.8, pp.8442-8456, 2012.

Ahmed Taha Hussein received a B.Sc. (First Class Hons.) in electronic and electrical engineering from the University of Mosul, Iraq, in 2006 and an M.Sc. degree (with distinction) in communication systems from the University of Mosul, Iraq, in 2011. He is a Higher Committee for Education Developments in Iraq (HCED) Scholar and is currently working toward a Ph.D. degree in the school of Electronic and Electrical Engineering, University of Leeds, Leeds, UK.

Prior to his Ph.D. study, he worked as a Communication Instructor in Electronic and Electrical Engineering Department in the College of Engineering, University of Mosul, Iraq from 2006 to 2009. He also worked as a lecturer in the Electronic and Electrical Engineering Department in the College of Engineering, University of Mosul, Iraq from 2011 to 2012. His research interests include performance enhancement techniques for visible light communication systems, visible light communication system design and indoor visible light communication networking.

Prof. Jaafar M. H. Elmirghani is the Director of the Institute of Integrated Information Systems within the School of Electronic and Electrical Engineering, University of Leeds, UK. He joined Leeds in 2007 and prior to that (2000–2007) as chair in optical communications at the University of Wales Swansea he founded, developed and directed the Institute of Advanced Telecommunications and the Technium Digital (TD), a technology incubator/spin-off hub. He has provided outstanding leadership in a number of large research projects at the IAT and TD. He received the Ph.D. in the synchronization of optical systems and optical receiver design from the University of Huddersfield UK in 1994 and the DSc in Communication Systems and Networks from University of Leeds, UK, in 2014. He has co-authored Photonic switching Technology: Systems and Networks, (Wiley) and has published over 400 papers. He has research interests in optical systems and networks. Prof. Elmirghani is Fellow of the IET, Fellow of the Institute of Physics and Senior Member of IEEE. He was Chairman of IEEE Comsoc Transmission Access and Optical Systems technical committee and was Chairman of IEEE Comsoc Signal Processing and Communications Electronics technical committee, and an editor of IEEE Communications Magazine. He was founding Chair of the Advanced Signal Processing for Communication Symposium which started at IEEE GLOBECOM'99 and has continued since at every ICC and GLOBECOM. Prof. Elmirghani was also founding Chair of the first IEEE ICC/GLOBECOM optical symposium at GLOBECOM'00, the Future Photonic Network Technologies, Architectures and Protocols Symposium. He chaired this Symposium, which continues to date under different names. He was the founding chair of the first Green Track at ICC/GLOBECOM at GLOBECOM 2011, and is Chair of the IEEE Green ICT committee within the IEEE Technical Activities Board (TAB) Future Directions Committee (FDC), a pan IEEE Societies committee responsible for Green ICT activities across IEEE, 2012-2015. He is and has been on the technical program committee of 33 IEEE ICC/GLOBECOM conferences between 1995 and 2014 including 14 times as Symposium Chair. He received the IEEE Communications Society Hal Sobol award, the IEEE Comsoc Chapter Achievement award for excellence in chapter activities (both in 2005), the University of Wales Swansea Outstanding Research Achievement Award, 2006, the IEEE Communications Society Signal Processing and Communication Electronics outstanding service award, 2009 and a best paper award at IEEE ICC'2013. He is currently an editor of: IET Optoelectronics, Journal of Optical Communications, IEEE Communications Surveys and Tutorials and IEEE Journal on Selected Areas in Communications series on Green Communications and Networking. He is Co-Chair of the GreenTouch Wired, Core and Access Networks Working Group, an adviser to the Commonwealth Scholarship Commission, member of the Royal Society International Joint Projects Panel and member of the Engineering and Physical Sciences Research Council (EPSRC) College. He has been awarded in excess of £22 million in grants to date from EPSRC, the EU and industry and has held prestigious fellowships funded by the Royal Society and by BT. He is an IEEE Comsoc Distinguished Lecturer 2013-2016.